The Central Role of Broken Bond-Bending Constraints in Promoting Glass Formation in the Oxides

M. Zhang and P. Boolchand*

A glass network of N atoms with n_1 of the atoms with a coordination number of 1, and m_2 of the atoms with a coordination number of 2 about which the bond-angle constraint is broken, will in general display a stiffness threshold (rigidity percolation threshold) when the average coordination increases to a critical value $\langle r\rangle_c = 2.4 - 0.4\,(n_1 - m_2)/N$. Silica and sodium tellurate glasses provide model examples for which this general relation predicts the observed rigidity percolation threshold; this relation predicts the percolation threshold only if one includes broken bond-bending constraints due to bridging oxygen in the former network and nonbridging oxygen in the latter network. The rigidity percolation threshold in $(Na_2O)_x(TeO_2)_{1-x}$ glasses is observed to occur near $x \simeq 0.18$ in tellurium-125 Lamb-Mössbauer factor measurements.

Telluria (TeO_2) and silica (SiO_2) consist of networks in which the cations (Te, Si) are fourfold-coordinated and the anion (O) is twofold-coordinated. Trigonal bipyramid $Te(O_{1/2})_4$ units (*1*) with a lone pair in the equatorial plane and tetrahedral $Si(O_{1/2})_4$ units form the building blocks of respective crystalline (and glassy) networks (Fig. 1, A and C). In both cases bridging oxygen sites serve as linkages between building blocks. Remarkably, although silica is the archetypal glass former (*2*), telluria, which has the same average coordination number, is the antithesis (*3*) of silica. However, alkali-oxide alloying in telluria produces nonbridging oxygen (NBO) and pronouncedly increases the glass-forming tendency (GFT) until, at $x \simeq 0.20$, $(Na_2O)_x(TeO_2)_{1-x}$ melts display (*3*) a GFT that parallels that of silica.

In this report we show that there is a common physical origin for this behavior in both silica and telluria that follows directly from Phillips constraint theory (*4*). Both SiO_2 melt and alkali tellurate melt near $x = 0.20$ are optimally constrained because the bond-angle constraint associated with bridging oxygen in the former, and with NBO in the latter, is broken. These considerations promote formation of strain-free polymerized networks and enhance the GFT at the stiffness, or rigidity percolation, threshold (*4*, *5*). These basic ideas provide a sound basis for understanding the microscopic origin of the unusual glass-forming tendency in silica, which has not been without controversies (*2*). Furthermore, these ideas also furnish a basis for understanding the generic role of alkali modifier atoms in enhancing the GFT in a variety of oxides. In this work we use an atomic-scale probe of rigidity, ^{125}Te Lamb-Mössbauer factors, to establish the rigidity percolation threshold in the tellurate glasses.

Fifteen years ago, Phillips (*4*) asserted that a network constrained by bond-stretching (α) and bond-bending (β) constraints sits at a mechanically critical point when the constraints per atom (n_c) equal the dimensionality or degrees of freedom (n_d) of the space in which it is embedded:

$$n_c = n_d \qquad (1)$$

These ideas were cast in the language of percolation theory by Thorpe (*5*), who showed that when atoms bond with a coordination number greater than or equal to 2, the number of zero-frequency modes (floppy modes) $F/N = n_d - n_c$ vanishes when the average coordination $\langle r\rangle$ acquires a critical value $\langle r\rangle_c = 2.40$.

Boolchand and Thorpe (*6*) extended constraint theory to include atoms with a coordination number of 1 and have shown that, in general, rigidity will percolate when the average coordination number of such a network approaches a critical value given by

$$\langle r\rangle_c = 2.4 - 0.4(n_1/N) \qquad (2)$$

provided atoms bond in conformity to the $8 - n$ rule, and the α and β constraints are held intact. The quantity n_1/N in Eq. 2 gives the fraction of atoms with a coordination number of 1.

Now let us consider the possibility that some (m_2/N) fraction of the atoms of the network with a coordination number of 2 have their β constraint broken. This is achieved by subtracting a term m_2/N from the enumeration of constraints performed earlier (*6*) by Boolchand and Thorpe. Consider a network of N atoms composed of n_r atoms that are r-fold–coordinated. In enumerating (*5*, *6*) constraints, we note that there are $r/2$ α constraints for a r-fold–coordinated atom. Furthermore, there are $2r - 3$ β constraints for an atom having $r \geq 2$, but zero (*6*) β constraints for an atom having $r = 1$. The average number of floppy modes per atom, F/N, in a three-dimensional network that has m_2 atoms twofold-coordinated with their β constraints broken, is given by

$$F/N = n_d - n_c$$

$$= 3 - \frac{\left[\sum_{r\geq 2} n_r(2r - 3 + r/2) + n_1/2 - m_2\right]}{N}$$

$$= 3 - \frac{\left[\sum_{r\geq 1} n_r[(5r/2) - 3] + n_1 - m_2\right]}{N}$$

$$= 6 - 5/2\langle r\rangle - (n_1 - m_2)/N \qquad (3)$$

where

$$\langle r\rangle = \sum_{r\geq 1} n_r r/N \text{ and } N = \sum_{r\geq 1} n_r \qquad (4)$$

We obtain the central result of the present work

$$\langle r\rangle = \langle r\rangle_c = 2.4 - 0.4(n_1 - m_2)/N \qquad (5)$$

when one requires F to vanish at the rigidity percolation threshold.

Silica is the illustrative example of Eq. 5. Both x-ray scattering (*7*) and ^{17}O nuclear quadrupole resonance spectroscopy (*8*) reveal a substantial spread ($\Delta\theta \sim 15°$) in the mean Si–O–Si bond angle $\theta \simeq 150°$. This provides for a flexibility in Si–O–Si linkages and the formation of a strain-free continuous network. For Si_xO_{1-x} alloys, if we take Si to be fourfold-coordinated and O to be twofold-coordinated, and the β constraint about all O sites to be broken, that is, $m_2/N = 1 - x$, and $n_1/N = 0$ (because there are no onefold-coordinated atoms), Eq. 5 requires

$$\langle r\rangle_c = 4x_c + 2(1 - x_c) = 2.4 + 0.4(1 - x_c)$$

or

$$x_c = 1/3 \qquad (6)$$

corresponding to the chemical composition SiO_2. The unusual GFT of SiO_2 is thus the direct consequence of the Phillips glass condition (*4*) being exactly satisfied when broken β constraints are taken into account. If we had ignored the broken β constraints associated with bridging oxygen sites in a Si_xO_{1-x} network, the glass condition would have been fulfilled at a lower value, $x_c = 0.20$.

Alkali tellurate glasses can also be described within the framework of Eq. 5. To understand the underlying behavior, one needs to decode the molecular structure of these glasses. The role of the alkali modifier in these glasses, as in the silicate glasses, consists in producing NBO sites, as suggest-

Department of Electrical and Computer Engineering, University of Cincinnati, Cincinnati, OH 45221, USA.

*To whom correspondence should be addressed.

ed by Raman scattering (9) and ^{125}Te Mössbauer hyperfine structure measurements (*10*). In the more open structure of the glasses, if we take Te, O, and Na to be four-, two-, and onefold-coordinated, respectively (conforming to the $8-n$ rule), then it is reasonable to expect that the NBO sites associated with the alkali modifier will display a range of Te–O–Na bond angles θ as illustrated in Fig. 1B. Thus, if we take the β constraint about NBO sites to be broken, that is, $m_2 = n_1 = 2x$, Eq. 5 for $(Na_2O)_x(TeO_2)_{1-x}$ glasses requires that

$$\langle r\rangle_c = [2x_c + 2x_c + 4(1 - x_c) + 4(1 - x_c)]/3$$
$$= 2.4 - 0.4(n_1 - m_2)/N(8 - 4x_c)/3 = 2.4$$

or

$$x_c = 0.20 \quad (7)$$

We thus find that alkali tellurate glasses satisfy the glass condition (*1*) at $x_c = 0.20$, provided β constraints associated with NBO sites are broken while those associated with bridging sites are held intact. The latter appears to be the case as revealed by neutron radial distribution function measurements (*11*) on tellurate glasses. If we had ignored the broken β constraints about NBO sites, on the other hand, the stiffness threshold would have been given by Eq. 2, and it would occur at a higher x_c value, $x_c = 0.25$.

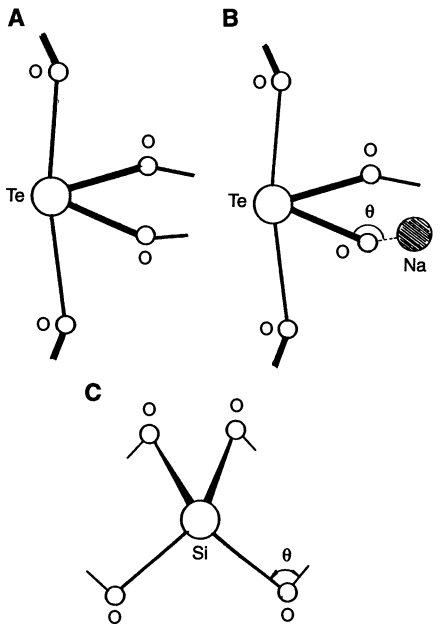

Fig. 1. (**A**) Diagram of a trigonal bipyramid $Te(O_{1/2})_4$ unit with a lone pair in the equatorial plane which serves as the building block of the TeO_2 network. (**B**) Sketch of the formation of Te–O^-–Na^+ linkages upon Na_2O alloying in telluria. A spread in the bond angle θ leads to the underlying bond-angle constraint for the nonbridging oxygen sites that is to be broken. (**C**) Schematic of a tetrahedral $Si(O_{1/2})_4$ unit, with the bridging oxygen bond angle θ constraint broken.

Scanning calorimetry measurements on these glasses have shown that the glass transition temperature T_g decreases systematically as a function of x (Fig. 2A), with the slope $|dT_g/dx|$ displaying a maximum near $x_c = 0.18$. Activation energy for enthalpy relaxation E_a, established from T_g variation as a function of scan rates, also displays a minimum (*12*, *13*) at $x_c = 0.18$ (Fig. 2B). Finally, ^{125}Te mean square displacement measurements at $T \to 0$ K, $\langle u_0^2\rangle$, extracted from our T-dependent Mössbauer effect measurements also show a discontinuity in slope near $x_c = 0.18$ (see Fig. 2C). We believe that the threshold behavior near $x_c = 0.18$ in each of the three observables has a common physical origin, representing the stiffness threshold in alkali tellurate glasses.

Convincing experimental evidence to suggest that the threshold at $x_c = 0.18$ is a stiffness threshold derives from our ^{125}Te mean square displacement measurements. In a soft or floppy network, one expects $\langle u_0^2\rangle/\lambda^2$ (where λ is the wavelength of the gamma ray) will be large, because atoms (or group of atoms) can be displaced from their equilibrium positions without much cost in energy, as a result of the presence of floppy modes (*5*). Just the reverse situation prevails in a rigid network, where a displacement of atoms from their equilibrium positions costs strain energy and leads in general to a smaller value of $\langle u_0^2\rangle/\lambda^2$. In this sense, $\langle u_0^2\rangle/\lambda^2$ provides a measure of network rigidity on a local (atomic) scale, as discussed in (*14*).

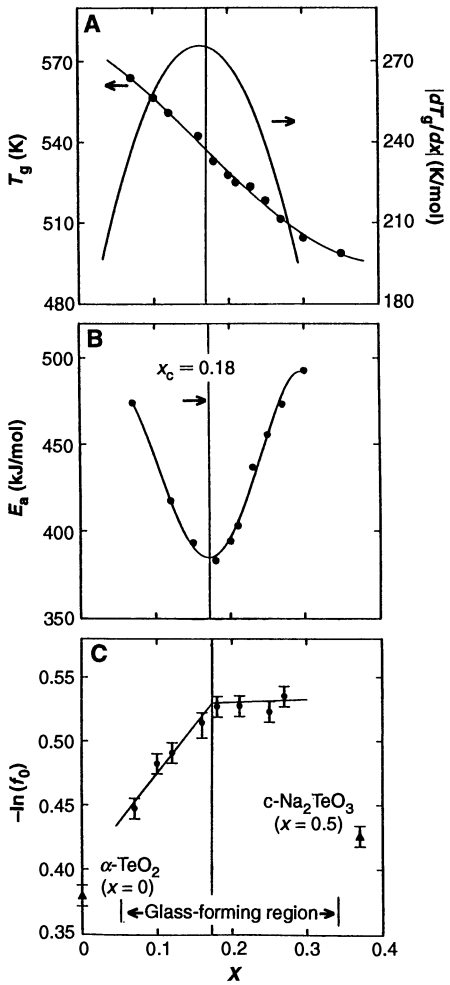

Fig. 2. Glass composition dependence of (**A**) T_g and the slope $|dT_g/dx|$, (**B**) E_a, activation energy for enthalpy relaxation, and (**C**) $\langle u_0^2\rangle$, ^{125}Te mean square displacement at $T = 0$ K in $(Na_2O)_x(TeO_2)_{1-x}$ glasses; plotted as $-\ln f_0 = \langle u_0^2\rangle/\lambda^2$, where f_0 is the recoil-free fraction as $T \to 0$ K. All plots display a threshold behavior at $x = x_c = 0.18$ (marked by vertical line), which we identify with the stiffness threshold; c-Na_2TeO_3, crystalline Na_2TeO_3.

To obtain Lamb-Mössbauer factors of a glass sample, we measured the complete T dependence (Fig. 3) of the integrated area under the resonance line shape in the range $12\text{ K} < T < 200$ K, using a vibration-free He closed-cycle cryostat (model Displex CS202 with DMX-20 shroud; APD Cryogenics, Allentown, Pennsylvania). A glass sample was cooled in the cryostat, and the nuclear resonance was excited with a $Mg_3Te^{125m}O_6$ emitter (*15*) held outside the cryostat at 300 K. In such a geometry, changes in the integrated area as a function of T derive from the recoil-free fraction $f(T)$ of the glass sample. The $f(T)$ variation was least squares–fitted to a Debye-like vibrational density of states to obtain the characteristic vibrational temperature, and thus, $f(T \to 0\text{ K}) = f_0 = \exp(-\langle u_0^2\rangle/\lambda^2)$. Trends in $\langle u_0^2\rangle$ as a function of glass composition (Fig. 2C) display a systematic softening (that is, an increase) with increasing molar content of Na_2O, with an apparent threshold near $x_c = 0.18$. Measurements on the crystalline phases, at $x = 0$ and $x = 1/2$, on the other hand, reveal a smaller mean square displacement $\langle u_0^2\rangle$ than in the glasses (see Fig. 2C), because α-TeO_2 and

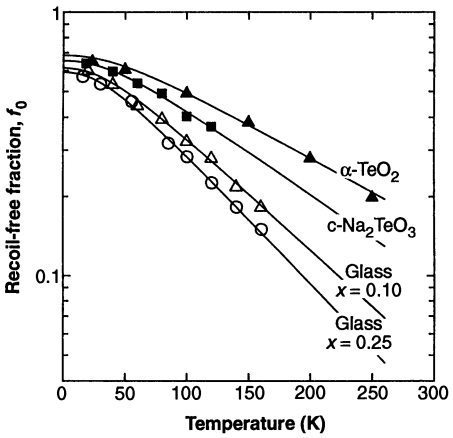

Fig. 3. Temperature dependence of the ^{125}Te recoil-free fraction in indicated $(Na_2O)_x(TeO_2)_{1-x}$ crystals (filled symbols) and glasses (open symbols). Data for selective glass compositions are shown.

Na_2TeO_3 represent examples of compacted and rigid crystalline networks.

Theoretically, $\langle u_0^2 \rangle$ provides a measure of the first inverse moment (*14*) of the vibrational density of states of a network, that is,

$$\langle 1/\omega \rangle = 2M \langle u_0^2 \rangle / 3\hbar \qquad (8)$$

where M is the mass of the resonant atom and h is Planck's constant. The sensitivity of $\langle 1/\omega \rangle$ to floppy modes in a network glass was recently demonstrated. Both neutron (*16*) and ^{119}Sn Mössbauer (*14*) vibrational density of states measurements showed a systematic reduction of $\langle 1/\omega \rangle$ as $\langle r \rangle$ increased to 2.4, with the appearance of a discontinuity (change in slope) near the stiffness threshold in binary Ge-Se glasses. The observed discontinuity in $\langle u_0^2 \rangle$ near $x_c = 0.18$ likewise constitutes evidence of a stiffness threshold in the tellurate glasses. This interpretation is independently confirmed by scanning calorimetry ($|dT_g/dx|$ and E_a) results (Fig. 2, A and B), which suggest that, near the privileged composition $x_c = 0.18$, these glasses are at a mechanically critical point, with a minimal configurational entropy change (*12*, *13*) occurring upon melting of the glass at T_g.

In tellurate glasses, the observed stiffness threshold ($x_c = 0.18$) is close to the predicted value ($x_c = 0.20$) based on Eq. 7, but it is significantly different from the predicted value ($x_c = 0.25$) based on Eq. 2. These results underscore the importance of including broken β constraints due to NBO sites in describing the stiffness threshold in the tellurate glasses.

In earlier discussions (*14*–*17*) of the stiffness threshold in chalcogenides, it was tacitly assumed that β constraints about the chalcogens were intact. The directionality of covalent interactions stems from the hybridization of *s* and *p* orbitals. Replacement of S or Se by the more electronegative O anion in a network leads to an increased transfer of charge from the cation (Si, Na) to the anion and to a weakening of angular or β forces about the O anion as ionic interactions grow at the expense of covalent ones. The unusual GFT displayed by some of the oxides undoubtedly arises as a result of these broken β constraints, as revealed by the convergence of constraint theory predictions with the results of measurements of the ^{125}Te Lamb-Mössbauer factors presented here.

REFERENCES AND NOTES

1. H. Beyer, *Z. Kristallogr.* **124**, 228 (1967); O. Lindquist, *Acta Chem. Scand.* **22**, 977 (1968).
2. W. H. Zachariasen, *J. Am. Chem. Soc.* **54**, 3841 (1932); J. C. Phillips, *Solid State Phys.* **37**, 93 (1982).
3. A. K. Yakhind, *J. Am. Ceram. Soc.* **49**, 670 (1966); J. E. Stanworth, *J. Soc. Glass Technol.* **36**, 217 (1952); *ibid.* **38**, 183 (1954).
4. J. C. Phillips, *J. Non Cryst. Solids* **34**, 153 (1979); *ibid.* **43**, 37 (1981).
5. M. F. Thorpe, *ibid.* **57**, 355 (1983); H. He and M. F. Thorpe, *Phys. Rev. Lett.* **54**, 2107 (1985).
6. P. Boolchand and M. F. Thorpe, *Phys. Rev. B* **50**, 10366 (1994).
7. R. L. Mozzi and B. E. Warren, *J. Appl. Crystallogr.* **2**, 164 (1969); R. J. Bell and P. Dean, *Philos. Mag.* **25**, 1381 (1972); R. Zallen, *The Physics of Amorphous Solids* (Wiley, New York, 1983), pp. 72–73.
8. P. J. Bray and M. L. Lui, in *Structure and Bonding in Non Crystalline Solids*, G. E. Walrafen and A. G. Revesz, Eds. (Plenum, New York, 1983), pp. 285–289.
9. T. Sekiya, N. Mochida, A. Ohtsuka, M. Tonokawa, *J. Non. Cryst. Solids* **144**, 128 (1992); J. Heo, D. Lang, G. H. Sigel, E. A. Mendoza, D. A. Hensley, *J. Am. Ceram. Soc.* **75**, 277 (1992).
10. M. Zhang, G. Anaple, W. Bresser, P. Boolchand, D. McDaniel, unpublished material.
11. S. Neov, I. Gerassimova, K. Krezhov, B. Sybzhimov, V. Kozhakharov, *Phys. Status Solidi A* **47**, 743 (1978).
12. M. Zhang, W. Bresser, P. Boolchand, *J. Non Cryst. Solids* **151**, 149 (1992).
13. M. Tatsumisago, B. L. Halfpap, J. L. Green, S. M. Lindsay, C. A. Angell, *Phys. Rev. Lett.* **64**, 1549 (1990).
14. P. Boolchand *et al.*, *Solid State Ionics* **39**, 81 (1990).
15. W. Bresser *et al.*, *Phys. Rev. B* **47**, 11663 (1993).
16. W. A. Kamitakahara *et al.*, *ibid.* **44**, 94 (1991).
17. G. H. Dohler, R. Dandoloff, H. Bilz, *J. Non Cryst. Solids* **42**, 87 (1980).

18. We acknowledge discussions with B. Goodman and D. McDaniel. This work was supported by NSF grant DMR-92-07166.

14 June 1994; accepted 22 September 1994

Nickel Oxide Interstratified α-Zirconium Phosphate, a Composite Exhibiting Ferromagnetic Behavior

Boris Shpeizer, Damodara M. Poojary, Kyungsoo Ahn, Charles E. Runyan Jr., Abraham Clearfield*

As part of an ongoing research program to synthesize novel pillared layered materials, nickel and cobalt hydroxyacetates were inserted between the layers of amine intercalates of α-zirconium phosphate. The structure of the resultant nickel composite, derived from x-ray powder data, was found to consist of a three-tiered layer of nickel atoms bridged by hydroxo and acetato groups. Heating to 420°C converted the hydroxyacetate layers to oxide and imparted ordered magnetic domains to the composite. The phosphate layers appear to act as a template directing the growth of the inserted layers in this class of composite materials.

Intercalation reactions of ions or molecules with layered solids are being used in novel ways to produce composites with useful properties such as ionic conduction, ion-exchange behavior, sorption, and catalysis (*1*, *2*). The pillaring of clays may be viewed as an ion-exchange intercalative reaction. Smectite clay minerals swell in water, and in the colloidal state they may exchange their interlamellar ions for inorganic polymers such as $[Al_{13}O_4(OH)_{24}(H_2O)_{12}]^{7+}$. Because of the low layer charge of the clay and the high charge of the inserting polymer, the resultant composite is porous. These pillared clays are under study as a new class of acidic catalysts (*3*–*5*).

Many layered compounds other than clays are theoretically amenable to pillaring. However, they generally have a high ratio of charge to surface area and therefore do not swell spontaneously. In order to induce pillaring, Clearfield and Roberts (*6*) first intercalated an amine into α-zirconium phosphate, $Zr(HPO_4)_2 \cdot H_2O$, and into other phosphates. This reaction increases the spacing between the inorganic sheets by formation of an amine bilayer that could then be replaced by the pillaring species. This procedure has now become a common technique for pillaring (*7*–*10*). We report here on a similar reaction that has yielded interstratified materials containing sheets of NiO or CoO between zirconium phosphate layers; the resulting NiO composite is ferromagnetic.

To prepare the composite, we first intercalated crystalline α-zirconium phosphate with either hexylamine or octylamine. The resultant interlayer spacings were 22.9 and 28.7 Å, respectively. These intercalates were then mixed with solutions of $Ni(OOCCH_3)_2 \cdot 4H_2O$ or mixtures of nickel nitrate and nickel acetate and refluxed for different lengths of time. The final products had interlayer spacings of 18.4 to 19.5 Å. A typical preparation involved dissolving 8.39 g of hexylamine (82.9 mmol) in 200 ml of water and then adding 10 g of solid crystalline α-zirconium phosphate (33.1 mmol). The mixture was stirred for 24 hours at room temperature. The solid phase was filtered off and washed extensively with doubly distilled water and a final wash with 50 ml of

Department of Chemistry, Texas A&M University, College Station, TX 77843, USA.

*To whom correspondence should be addressed.